JOURNAL OF MATERIALS SCIENCE 33 (1998) 1309–1317

Oxidation mechanism of Si_3N_4-bonded SiC ceramics by CO, CO_2 and steam

G. X. WANG*, G. Q. (MAX) LU[+§], BENYAN PEI[‡], A. B. YU*
*School of Materials Science and Engineering, University of New South Wales, Sydney, NSW 2052, Australia
[+] Department of Chemical Engineering, University of Queensland, Brisbane, Qld 4072, Australia
[‡] Division of Process Metallurgy, Lulea University of Technology, 97187 Lulea, Sweden

This paper presents a theoretical and experimental investigation into the oxidation reactions of Si_3N_4-bonded SiC ceramics. Such ceramics which contain a small amount of silicon offer increased oxidation and wear resistance and are widely used as lining refractories in blast furnaces. The thermodynamics of oxidation reactions were studied using the JANAF tables. The weight gain was measured using a thermogravimetric analysis technique to study the kinetics. The temperature range of oxidation measurements is from 1073 to 1573 K and the oxidation atmosphere is water vapour, pure CO and CO–CO_2 gas mixtures with various CO-to-CO_2 ratios. Thermodynamic simulations showed that the oxidation mechanism of Si_3N_4-bonded SiC ceramics is passive oxidation and all components contribute to the formation of a silica film. The activated energies of the reactions follow the sequence $Si_3N_4 > SiC > Si$. The kinetic study revealed that the oxidation of Si_3N_4-bonded SiC ceramics occurred in a mixed regime controlled by both interface reaction and diffusion through the silica film. Under the atmosphere conditions prevailing in the blast furnace, this ceramic is predicted to be passively oxidized with the chemical reaction rate becoming more dominant as the CO concentration increases.

Nomenclature

A_0	frequency factor defined by Equation 32 (h^{-1})
D_{CO}, D_{CO_2}, D_{H_2O}, D_{SiO}	diffusion coefficients of CO, CO_2 H_2O(g) and SiO(g) molecules, respectively, ($m^2\ s^{-1}$)
E	activation energy for a given reaction, (kJ mol^{-1})
ΔG^0	standard Gibbs energy change (kJ)
k_c, k_d, k_m	rate constants corresponding to the chemical reaction, diffusion and mixed rate-controlling mechanisms, respectively (h^{-1})
P_{CO}, P_{CO_2}	CO and CO_2 partial pressures, respectively, in the blast furnace (atm)
P_{N_2}	N_2 partial pressure in a given reaction system (atm)
$P_{CO,tr}$, $P_{CO_2,tr}$, $P_{H_2O,tr}$	active–passive transition partial pressures of CO, CO_2 and H_2O(g), respectively, for the oxidation of Si, SiC and Si_3N_4 in pure CO, CO–CO_2 gas mixtures and steam (atm)
$P_{CO,eq}$, $P_{SiO,eq}$	equilibrium CO and SiO(g) partial pressures, respectively, for the reactions of Si, SiC and Si_3N_4 with SiO_2 (atm)
R	gas constant, equal to 8.314×10^{-3} kJ $mol^{-1}\ K^{-1}$
t	reaction time (h)
T	temperature (K)
W_0, W_t, W_∞	weights for the given specimen at the initial, time t and final stages, respectively (gf)
W_{Si}, W_{SiC}, $W_{Si_3N_4}$	weight percentages of Si, SiC and Si_3N_4 in the given specimen (wt%)
$\Delta W(t)$	weight gain for the given specimen at any time t (gf)
X	fractional conversion defined by Equation 28 (%)
α	transition coefficient relative to the Si-based components in Si_3N_4-bonded SiC ceramics
φ^2	Thiele modulus defined by Equation 31b

§ To whom all correspondence should be addressed. e-mail. maxlu@cheque.uq.edu.au.

1. Introduction

Silicon-carbide-based refractories were first introduced into blast furnaces in the late 1960s [1]. Compared with other oxide refractories, SiC bricks are typified by low porosity, high abrasion-resistant strength, good alkali and thermal shock resistances and high thermal conductivity [2]. Si_3N_4-bonded SiC bricks containing approximately 20–25 wt% Si_3N_4 and small amounts of silicon are the major type of silicon carbide used in blast furnaces. In the severe wear zones of the blast furnace, one major wear factor is oxidation of the bricks by air, carbon dioxide (CO_2), carbon monoxide (CO) and water vapour, which are present in certain zones of the refractory wall. Understanding the oxidation behaviour is of importance to achieve longer service life for SiC bricks and to improve product quality.

The oxidation of such material in air has been previously studied and reported [3]. As expected, the oxidation of Si_3N_4-bonded SiC bricks exhibits similar behaviour to the oxidation of pure SiC or Si_3N_4 (see [3] and references cited therein). The oxidation is controlled by both reaction at the interface and diffusion through the product layer. Moreover, a few studies have also been reported on the oxidation of SiC bricks by CO, CO_2 and water vapour [2, 4]. Keran and Brown [2] and Kaufman *et al.* [4] reported volume expansion of their products when subjected to steam oxidation. They further discussed the range of sensitivity of their products to these oxidizing species. However, there is no study reported on the oxidation of Si_3N_4-bonded SiC bricks by CO, CO_2 and water vapour in terms of thermodynamics and kinetics.

The present work is a continuation of our previous work [3]. We intend to study the oxidation of Si_3N_4-bonded SiC bricks by CO, CO_2 and H_2O(g) both thermodynamically and kinetically. The temperature range of the study is from 1073 to 1573 K. Water vapour and CO–CO_2 gas mixtures with different CO–CO_2 ratios were chosen as the oxidant species in the experimental work, which was carried out by measuring the weight gain during passive oxidation. The stability of such bricks will be discussed with respect to active and passive oxidation under the gas environments that were present within the refractory walls of blast furnaces from the bosh to the upper stack. The transitions between active and passive oxidation will be analysed for various oxidant reagents. A kinetic model of unreacted core will be used to discriminate between the rate mechanisms by fitting to the weight gain versus time data.

2. Theory

2.1. Thermodynamic analysis

Similar to the case with air oxidation [3], the following thermodynamic analysis is made for the oxidation of SiC, Si_3N_4 and metallic Si. The latter is a major impurity in the bricks. The Gibbs energy data for α-SiC, α-Si_3N_4 and high-cristobalite SiO_2 from the JANAF tables [5] are used in the following analysis. The different forms of oxidation product SiO_2 are not distinguished, as the differences between the Gibbs energy data for the different forms of SiO_2 are negligibly small (within $\pm$ 4 kJ mol^{-1}). The Gibbs energy data of SiO(g), CO, CO_2 and H_2O(g) are also taken from the JANAF tables [5].

Only a few thermodynamic analyses exist in the literature on the stability of Si, SiC and Si_3N_4 upon oxidation by CO–CO_2 mixture [6, 7] and by H_2O(g) [7]. According to these studies, the stabilities of Si, SiC and Si_3N_4 in these oxidizing atmospheres depend mainly on the stability of the oxidation product, SiO_2. This means that the stability of Si_3N_4-bonded SiC bricks in a blast furnace depends essentially on the oxidation protective layer, i.e., the SiO_2 scale. Similar to air oxidation, Si-based materials may be oxidized either passively or actively by CO, CO_2 or H_2O(g) at high temperatures, depending on these oxidant potentials. Thermodynamic calculations were first carried out by means of the SOLGASMIX program [8] to determine the predominant gaseous species at the solid–gas interface. From the calculations, the different reactions with CO, CO_2 and H_2O(g) as oxidants are discussed as follows.

2.1.1. Active oxidation

If the oxidant potentials are low, active oxidation with the formation of SiO(g) vapour occurs according to the following reactions in the temperature range 1073–1573 K:

(a) *With CO as oxidant*,

$$Si + CO = SiO(g) + C$$

$$\Delta G^0 = 13.523 - 0.047T + 0.015T \log T \quad (1)$$

$$SiC + CO = SiO(g) + 2C$$

$$\Delta G^0 = 84.943 - 0.055T + 0.015T \log T \quad (2)$$

$$Si_3N_4 + 3CO = 3SiO(g) + 2N_2 + 3C$$

$$\Delta G^0 = 786.460 - 0.473T + 0.046T \log T \quad (3)$$

(b) *With CO_2 as oxidant*,

$$2Si + CO_2 = 2SiO(g) + C$$

$$\Delta G^0 = 197.437 - 0.268T + 0.031T \log T \quad (4)$$

$$2SiC + CO_2 = 2SiO(g) + 3C$$

$$\Delta G^0 = 340.277 - 0.284T + 0.031T \log T \quad (5)$$

$$2Si_3N_4 + 3CO_2 = 6SiO(g) + 4N_2 + 3C$$

$$\Delta G^0 = 2084.090 - 1.468T + 0.092T \log T \quad (6)$$

(c) *With H_2O(g) as oxidant*,

$$Si + H_2O(g) = SiO(g) + H_2$$

$$\Delta G^0 = 147.375 - 0.189T + 0.015T \log T \quad (7)$$

$$SiC + 2H_2O(g) = SiO(g) + CO + 2H_2$$

$$\Delta G^0 = 352.647 - 0.338T + 0.015T \log T \quad (8)$$

$$Si_3N_4 + 3H_2O(g) = 3SiO(g) + N_2 + 3H_2$$

$$\Delta G^0 = 1188.016 - 0.898T + 0.046T \log T \quad (9)$$

Here ΔG^0 (kJ) is the standard Gibbs energy change and T (K) is the temperature. Under active oxidation, the bare surface of Si, SiC and Si_3N_4 is exposed and materials continuously deteriorate owing to the formation of SiO(g).

2.1.2. Passive oxidation

In environments with high oxidant potentials, passive oxidation results:

(a) *With CO as oxidant*,

$$Si + 2CO = SiO_2 + 2C$$

$$\Delta G^0 = -680.980 + 0.349T \quad (10)$$

$$SiC + 2CO = SiO_2 + 3C$$

$$\Delta G^0 = -609.560 + 0.341T \quad (11)$$

$$Si_3N_4 + 6CO = 3SiO_2 + 2N_2 + 6C$$

$$\Delta G^0 = -1297.050 + 0.716T \quad (12)$$

(b) *With CO_2 as oxidant*,

$$Si + CO_2 = SiO_2 + C$$

$$\Delta G^0 = -510.59 + 0.176T \quad (13)$$

$$SiC + CO_2 = SiO_2 + 2C$$

$$\Delta G^0 = -439.170 + 0.168T \quad (14)$$

$$Si_3N_4 + 3CO_2 = 3SiO_2 + 2N_2 + 3C$$

$$\Delta G^0 = -785.880 + 0.195T \quad (15)$$

(c) *With $H_2O(g)$ as oxidant*,

$$Si + 2H_2O(g) = SiO_2 + 2H_2$$

$$\Delta G^0 = -413.276 + 0.066T \quad (16)$$

$$SiC + 3H_2O(g) = SiO_2 + 3H_2 + CO$$

$$\Delta G^0 = -96.144 + 0.005T \quad (17)$$

$$Si_3N_4 + 6H_2O(g) = 3SiO_2 + 6H_2 + 2N_2$$

$$\Delta G^0 = -493.938 - 0.133T \quad (18)$$

Passive oxidation is characterized by weight gain due to the formation of solid SiO_2 product scale. This prevents further oxidation of Si, SiC and Si_3N_4. The usefulness of SiC bricks depends not only on their intrinsic stability but also on the stability of this protective oxide layer.

2.1.3. Transition from passive to active oxidation

Except in the case of oxidation of SiC with CO and CO_2, the transition from passive to active oxidation can occur by consumption of SiO_2 which reacts with the substrates Si, SiC and Si_3N_4 according to the following reactions:

$$Si + SiO_2 = 2SiO(g)$$

$$\Delta G^0 = 708.027 + 0.031T \log T - 0.444T \quad (19)$$

$$SiC + 2SiO_2 = 3SiO(g) + CO$$

$$\Delta G^0 = 1473.950 + 0.046T \log T - 0.848T \quad (20)$$

$$Si_3N_4 + 3SiO_2 = 6SiO(g) + 2N_2$$

$$\Delta G^0 = 2869.970 + 0.092T \log T - 1.662T \quad (21)$$

For the case where SiC is oxidized by CO and CO_2, the transition is governed by the following reaction:

$$SiC + SiO_2 = SiO(g) + C$$

$$\Delta G^0 = 779.447 - 0.451T + 0.031T \log T \quad (22)$$

The transition between active and passive oxidations has been studied both thermodynamically and kinetically for the case of air oxidation [3]. The kinetic studies took into account the mass-transfer constraints and determined the transition point in terms of oxygen potentials in the bulk gas for given temperatures. For the case with CO, CO_2 and $H_2O(g)$ as oxidants, there is no such study available in the literature.

If CO is used as an oxidant, following the concept of O_2 oxidation [3, 9] and considering the oxygen balance, it is straightforward to get the following to determine the transition pressure $P_{CO,tr}$:

$$P_{CO,tr} = \left(\frac{D_{SiO}}{D_{CO}}\right)^{1/2} P_{SiO,eq} = 0.69 P_{SiO,eq} \quad (23)$$

where $P_{CO,tr}$ (atm) is the active–passive transition CO partial pressure, corresponding to the oxidation of Si, SiC and Si_3N_4 in a CO atmosphere. $P_{SiO,eq}$ (atm) is the equilibrium SiO(g) partial pressure for the reactions of Si, SiC and Si_3N_4 with SiO_2. D_{SiO} ($m^2\ s^{-1}$) and D_{CO} ($m^2\ s^{-1}$) are the diffusion coefficients of SiO(g) and CO molecules, respectively. The $P_{SiO,eq}$ values are determined from Equations 19, 21 and 22 for Si, Si_3N and SiC, respectively.

The diffusivities can be calculated by the Shapman–Enskog theory [10] and D_{SiO}/D_{CO} was estimated to be 0.48 at 1500 K in the present study. Values of the Lennard-Jones parameters, the integral collision and diffusivity at 1500 K are given in Table 1.

In the case when CO_2 is the oxidant, the following equation can be used to determine the transition CO_2 partial pressures if oxygen balance is considered:

$$P_{CO_2,tr} = 0.5\left(\frac{D_{SiO}}{D_{CO_2}}\right)^{1/2} P_{SiO,eq} = 0.39 P_{SiO,eq} \quad (24)$$

where $P_{CO_2,tr}$ (atm) is the active–passive transition CO_2 partial pressure respectively for the oxidation of Si, SiC and Si_3N_4 in a CO_2 atmosphere. D_{CO_2} ($m^2\ s^{-1}$) is the diffusion coefficient of CO_2 molecules. The $P_{SiO,eq}$ values are also determined from Equations 19, 21 and 22 for Si, Si_3N_4 and SiC, respectively. D_{SiO}/D_{CO_2} was estimated to be 0.62 at 1500 K.

Finally if $H_2O(g)$ is used as the oxidant, the following equations can be applied to determine the

TABLE I Values of the Lennard-Jones parameters, the integral collision and diffusion coefficient at 1500 K (from Bird *et al.* [10]) where $\sigma_{ij} = (\sigma_i + \sigma_j)/2$ and $D_{ij} = 0.001\,858\,3[(1/M_i + 1/M_j)T^3]^{1/2}/(P\sigma_{ij}^2\Omega_{ij})$

i	j	σ_i (nm)	σ_{ij} (nm)	Ω_{ij}	D_{ij} ($cm^2\,s^{-1}$)
SiO	N_2	0.478[a]	0.423	(1.00)[a]	1.46
CO	N_2	0.359	0.364	0.7139	3.05
O_2	N_2	0.343	0.356	0.7167	3.08
CO_2	N_2	0.388	0.378	0.7731	2.36
H_2O[b]	N_2	0.351	0.359	0.949	2.67
SiO	Air	0.478	0.420	(1.00)[a]	1.46
CO	Air	0.359	0.361	0.7139	3.07
CO_2	Air	0.388	0.375	0.7731	2.38
O_2	Air	0.343	0.353	0.7167	3.10
H_2O[b]	Air	0.3505	0.356	0.949	2.69
N_2		0.368			
Air		0.362			

[a] From Balat *et al.* [11]
[b] For H_2O, $T_C = 374.1\ ^\circ C = 647.1$ K, $P_C = 218.3$ atm, $\varepsilon/k = 0.77T_C = 498.27$ and $\sigma = 2.44(T_C/P_C)^{1/3} = 3.505$.

transition $H_2O(g)$ partial pressures:

$$P_{H_2O,tr} = \left(\frac{D_{SiO}}{D_{H_2O}}\right) P_{SiO,eq} = 0.74P_{SiO,eq} \quad \text{(for Si and } Si_3N_4\text{)} \quad (25)$$

$$P_{H_2O,tr} = \left(\frac{D_{SiO}}{D_{H_2O}}\right)^{3/8}\left(\frac{D_{CO}}{D_{H_2O}}\right)^{1/8} P_{SiO,eq}^{3/4}P_{CO,eq}^{1/4} = 0.81P_{SiO,eq}^{3/4}P_{CO,eq}^{1/4} \quad \text{(for SiC)} \quad (26)$$

where $P_{H_2O,tr}$ (atm) is the active–passive transition $H_2O(g)$ partial pressure for the oxidation of Si, SiC and Si_3N_4 in steam. D_{H_2O} ($m^2\,s^{-1}$) is the diffusion coefficient of $H_2O(g)$ molecules. The $P_{SiO,eq}$ values are determined from Equations 19, 21 and 20 for Si, Si_3N_4 and SiC, respectively, whereas $P_{CO,eq}$ is determined from Equation 20 for SiC. D_{SiO}/D_{H_2O} and D_{CO}/D_{H_2O} were estimated to be 0.55 and 1.14, respectively, at 1500 K.

2.2. Kinetics of oxidation

On the assumption that the three components are oxidized stoichiometrically, it is not difficult to demonstrate from Equations 10–18 that the final weight of a specimen upon complete oxidation is

$$W_\infty = 60W_0\left(\frac{W_{SiC}}{40} + 3\,\frac{W_{Si_3N_4}}{140} + \frac{W_{Si}}{28}\right) = \alpha W_0 \quad (27)$$

where W_0 (gf) is the initial weight of the specimen. W_{SiC} (wt%), $W_{Si_3N_4}$ (wt%) and W_{Si} (wt%) are the weight percentages of SiC, Si_3N_4 and Si, respectively in Si_3N_4-bonded SiC ceramics. α is a constant (equal to 1.369 for the samples studied here). The amount of weight losses due to emissions of C and N from SiC and Si_3N_4 were found to be insignificant and were therefore neglected in Equation 27. Define the fractional conversion X, in terms of SiO_2 formation during the oxidation process, at any time t as follows:

$$X = \frac{W_t - W_0}{W_\infty - W_0} = \frac{1}{\alpha}\frac{\Delta W(t)}{W_0} \quad (28)$$

where W_t and $\Delta W(t)$ are the weight and weight gain, respectively, of the specimen at any time t. The conversion versus time data were obtained from the oxidation experiments and are expected to follow one of the kinetic models of Szekely *et al.* [12], depending on the rate-controlling mechanisms. For isothermal and constant specimen size processes, there are generally three kinetic expressions [12].

If the chemical reaction is the controlling mechanism at the surface of a shrinking core, then

$$1 - (1 - X)^{1/n} = k_c t \quad (29)$$

where $n = 1$, 2 and 3 for a long slab, a cylinder and a sphere, respectively. $n = 3$ in this study because of the spherical particle assumption.

For diffusion control through the product layer,

$$1 - 3(1 - X)^{2/3} + 2(1 - X) = k_d t \quad (30)$$

For mixed control due to reaction at the interface and diffusion through the product layer,

$$1 - (1 - X)^{1/3} + \varphi^2[1 - 3(1 - X)^{2/3} + 2(1 - X)] = k_m t \quad (31a)$$

where $k_c(h^{-1})$, $k_d(h^{-1})$ and $k_m(h^{-1})$ are the rate constants for the three control mechanisms, respectively. φ^2 is the Thiele modulus defined as follows:

$$\varphi^2 = \frac{k_m V_p(1 + 1/K_E)}{2D_e A_p} \quad (31b)$$

where V_p and A_p are the volume and surface area, respectively, of the particle, K_E is the equilibrium reaction constant and D_e is the effective diffusivity in through the product layer. It is obvious that φ^2 represents the ratio of the chemical reaction rate to the diffusion rate. A large value for this ratio (much greater than 1) means that the oxidation is diffusion controlled with a relatively fast interface reaction.

The appropriate rate expression can be determined by fitting the conversion–time data, obtained under the given oxidation experiments, to each of the above equations. For this purpose, a standard curve fitter, i.e., the Marquardt–Levenberg algorithm, was employed in this work. The temperature dependence of the rate constants was examined using the Arrhenius law

$$k = A_0 \exp\left(-\frac{E}{RT}\right) \quad (32)$$

where $k(h^{-1})$ is the rate constant corresponding to k_c, k_d or k_m for the given rate-controlling mechanisms. R is the gas constant, i.e., $R = 8.314 \times 10^{-3}$ kJ $mol^{-1}\,K^{-1}$. Using Equation 32 to fit the experimental data can result in kinetic parameters such as activation energy E (kJ mol^{-1}) and frequency factor A_0 (h^{-1}).

3. Experimental procedure

The oxidation of Si_3N_4-bonded SiC bricks in air and water vapour and gas mixture of CO/CO_2 with different compositions was investigated. The experimental results of air oxidation have been reported elsewhere [3]. The Si_3N_4-bonded SiC brick samples have the dimensions 10 mm × 10 mm × 20 mm. The bricks contain about 71 wt% SiC, 22 wt% Si_3N_4, 2 wt% SiO_2 and 1 wt% Si (on average). The Fe content accounts for less than 1 wt% in the form of Fe_2O_3. The apparent porosity is about 18% and the solid density is 2981 kg m^{-3} [11]. In order to reduce the experimental error attributed to inhomogeneity of the bricks, two brick samples were used at the same time for each oxidation experiment.

The experiments were carried out in an electrical furnace. The furnace was heated at a rate of about 8 °C min^{-1} to the desired temperature while Ar gas was passed through the furnace as a purge gas. After the desired temperature (1073–1573 K) was reached, the Ar gas was stopped and oxidant gas was introduced. After a certain time of oxidation, the specimen was discharged from the furnace upon cooling to room temperature. Each specimen was then weighed using an analytical balance (TG328A) with an accuracy of about 10^{-5} gf. An average value of the weight gains of the two specimens was taken.

Oxidation runs with water vapour were conducted in a steam stream. For oxidation with $CO–CO_2$ gas mixtures, technically pure CO_2 gas was dried by passing through a packed bed with glass fibre and P_2O_5 powder. CO gas was generated by reacting CO_2 with charcoal at about 1373 K and then passing through acid $C_6H_3(OK)_3$ to absorb O_2 and further through KOH solution to remove CO_2. Purified CO gas was further passed through a heating furnace filled with copper turnings at about 873 K to remove trace O_2 and then through dry P_2O_5 to remove moisture. The flow rates of CO and CO_2 were adjusted by capillary flowmeters to give different $CO–CO_2$ ratios before the gas entering the oxidation furnace. All experimental conditions are listed in Table II. A $CO–CO_2$ ratio of approximately 3 to 1 represents the condition in the blast furnace.

4. Results and discussion

The thermodynamic calculations using the JANAF tables are shown in Figs 1–3. In these figures, the active–passive transition oxidant pressures are shown for oxidations of Si, SiC and Si_3N_4 as functions of temperature. Figs 4–7 show the results obtained by oxidation experiments under the various conditions in which the solid curves are the predictions obtained by the kinetic model best fitted. Figs 8–10 below, indicate the effects of temperature and oxidants on the oxidation process, permitting the determination of the kinetic parameters for oxidation of Si_3N_4-bonded SiC ceramics.

4.1. Oxidation mechanism of Si_3N_4-bonded SiC ceramics

It is known that the stability of Si_3N_4-bonded SiC ceramics is essentially dependent on the oxidation mechanism, i.e., active or passive oxidation. In order to understand the oxidation behaviour of Si_3N_4-bonded SiC ceramics under different conditions, such

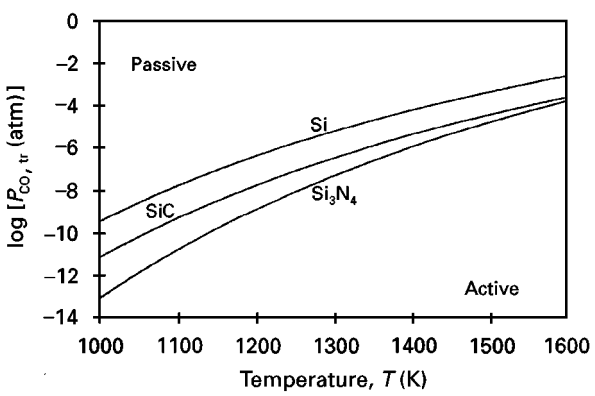

Figure 1 Transition CO pressures for oxidation of Si, SiC and Si_3N_4 (P_{N_2} = 1 atm).

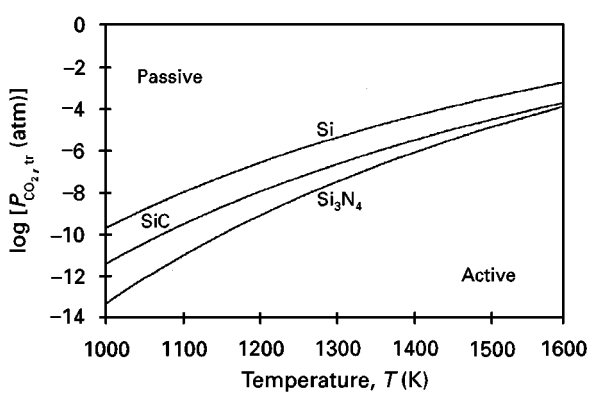

Figure 2 Transition CO_2 pressures for oxidation of Si, SiC and Si_3N_4 (P_{N_2} = 1 atm).

TABLE II Experimental conditions for the oxidation of SiC

Oxidant	Temperature (K)	Flow rate (cm^3 min^{-1})	Time (h)
H_2O(g)	1073–1573	4–5 (at 373 K)	12
Pure CO	1373–1573	400	12
$CO + CO_2$	1473	400	12
$CO–CO_2$ (CO-to-CO_2 ratio, 3 to 1) (a simulated blast furnace environment)	1373–1573	400	10

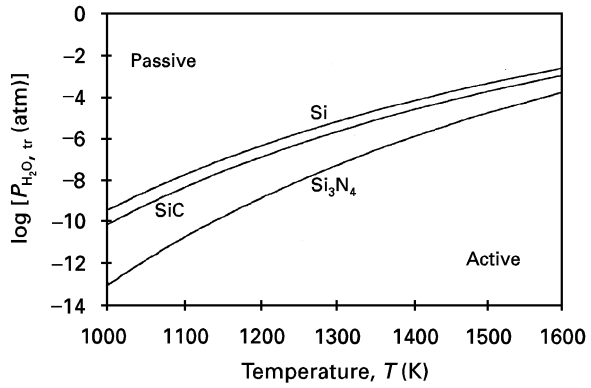

Figure 3 Transition H_2O(g) pressures for oxidation of Si, SiC and Si_3N_4 ($P_{N_2} = 1$ atm).

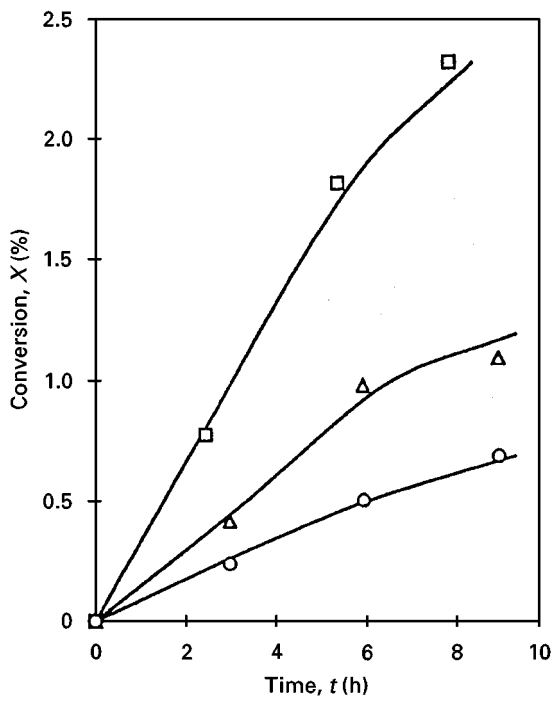

Figure 4 Conversion–time profiles fitted to a mixed rate-controlling equation for oxidation by pure CO at various temperatures. (□), 1573 K; (△), 1473 K; (○), 1373 K.

as the environment in a blast furnace, a thermodynamic analysis of the oxidations of pure Si, SiC and Si_3N_4 is first dealt with.

Comparing Figs 1–3, it can be seen that the sequence of the active–passive transition oxidant pressures is in the following order: Si > SiC > Si_3N_4. This is quite consistent with the results obtained by the previous studies on activation energies of the oxidation reactions. It has been shown from these studies [14, 15] that the activation energies are 119 kJ mol^{-1}, 134–498 kJ mol^{-1} and 300–400 kJ mol^{-1} for the oxidation reactions of Si, SiC and Si_3N_4, respectively, giving the reversed sequence from that of the transition oxidant pressures, i.e., Si_3N_4 > SiC > Si. This indicates that the free Si remaining in Si_3N_4-bonded SiC ceramics is more easily oxidized than SiC or Si_3N_4.

On the other hand, it is also seen from Figs 1–3 that the transition oxidant pressures only vary within

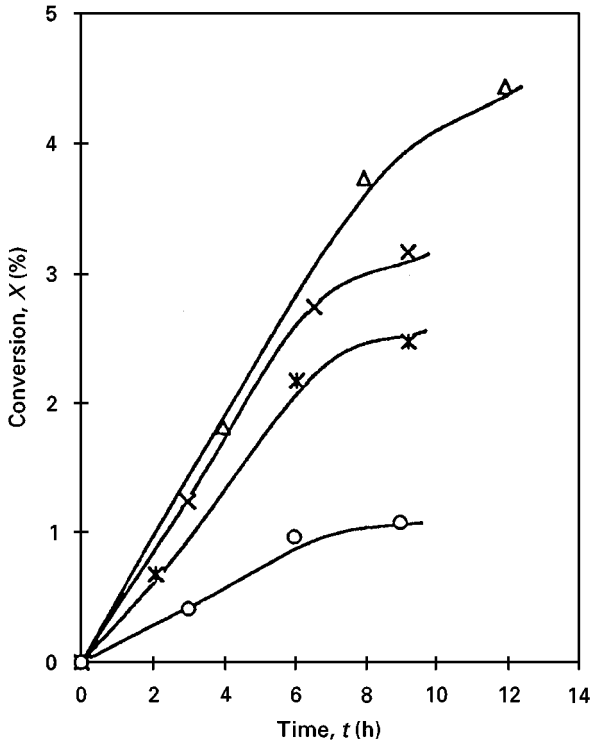

Figure 5 Conversion–time profiles fitted to a mixed rate-controlling equation for oxidation at 1473 K by CO–CO_2 gas mixtures with various CO-to-CO_2 ratios. (△), 0 to 4; (×), 1 to 3; (∗), 3 to 1; (○), 4 to 0.

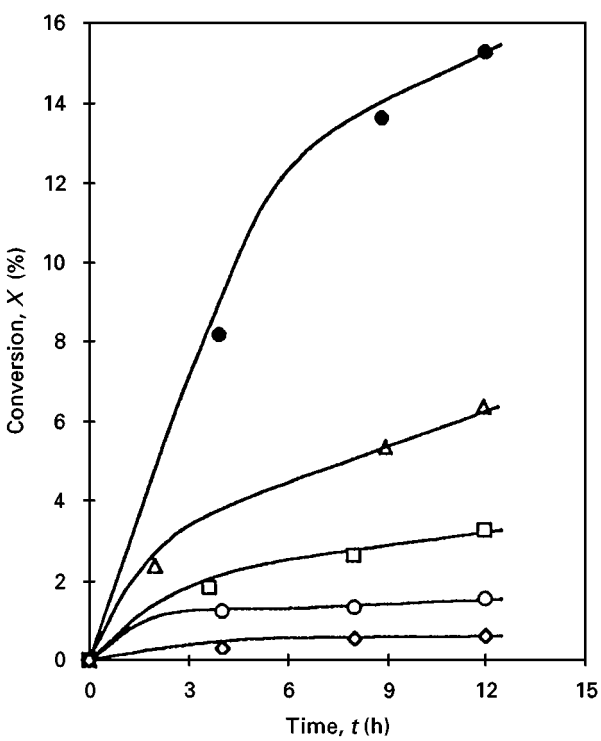

Figure 6 Conversion–time profiles fitted to a mixed rate-controlling equation for oxidation by H_2O(g) at various temperatures. (●), 1473 K; (△), 1373 K; (□), 1273 K; (○), 1173 K; (◇), 1073 K.

a small range (one order of magnitude) for the oxidation of Si, SiC and Si_3N_4, regardless of the oxidant type, i.e., CO, CO_2 or H_2O(g). This implies that all Si-based components in Si_3N_4-bonded SiC ceramics may be simultaneously oxidized in the form of either active or passive oxidation for a given condition. In

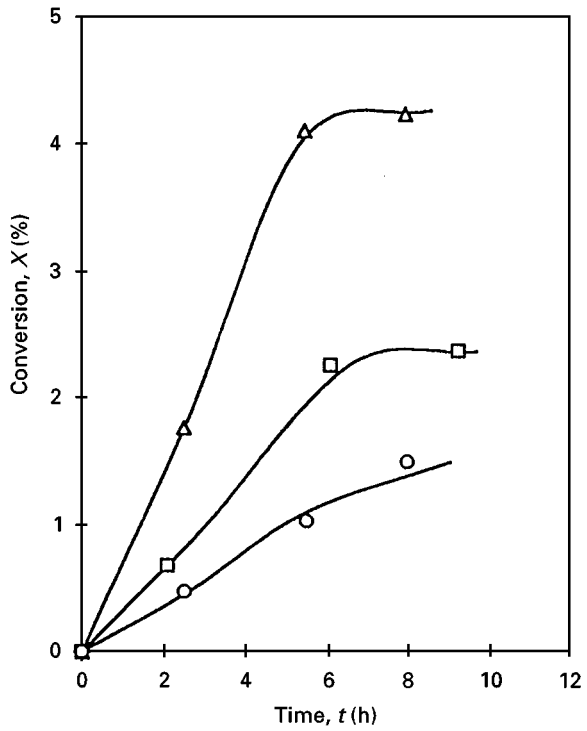

Figure 7 Conversion–time profiles fitted to a mixed rate-controlling equation for oxidation under the simulated blast furnace environment at various temperatures (CO-to-CO_2 ratio, 3 to 1). (△), 1573 K; (□), 1473 K; (○), 1373 K.

the blast furnace environment, the CO partial pressure, P_{CO}, and the CO_2 partial pressure, P_{CO_2}, are approximately estimated to be about 0.83 atm and 0.28 atm, respectively. Under these conditions Si, SiC and Si_3N_4 will be oxidized passively to SiO_2 by CO, CO_2 and water vapour based on the above thermodynamic analysis and all components contribute to the formation of the SiO_2 film. From an oxidation point of view, Figs 1–3 demonstrate that Si_3N_4-bonded SiC bricks can be used in a blast furnace with SiO_2 as a protection layer against further oxidation. However, species such as alkali vapour, and slag may erode the SiO_2 layer and make the bricks further oxidized and eroded. This is a topic for future work on the alkali erosion of SiC bricks.

By fitting the conversion–time data to Equations (29)–(31), it is found that Equation (31) gives the best fit to the experimental data available, i.e., the oxidation rate can be best presented by a mixed control due to reaction at the interface and diffusion through the product layer. Figs 4–7 show that the oxidation of Si_3N_4-bonded SiC bricks by H_2O(g), CO and CO–CO_2 gas mixtures in a given temperature range is under mixed control due to interface reaction and diffusion through the product layer. Fig. 7 shows the experimental results and the best-fit curves for the oxidation under a simulated blast furnace environment. Obviously, Si_3N_4-bonded SiC bricks used as blast furnace lining may be oxidized by the oxidants present in the furnace and the oxidation process is subject to the mixed rate-controlling mechanism. Similar oxidation kinetics were also observed by Luthra [16] for the oxidation of SiC and Si_3N_4.

4.2. Kinetic parameters of oxidation

As mentioned above, the mixed rate-controlling mechanism represents the overall rate process which is the best for oxidation of Si_3N_4-bonded SiC ceramics. The rate constant is expressed by Equation 31a and can be determined by the optimal fitting of the experimental data under various conditions to this equation. In the process of curve fitting, the Thiele modulus reflecting the ratio of chemical reaction rate to diffusion rate in the mixed rate is meanwhile obtained. These parameters, i.e., the rate constant and the Thiele modulus, are varied for various temperatures and oxidants.

Fig. 8 shows plots of the logarithms of the rate constants versus the reciprocal of temperature, for various oxidants. The intercepts and slopes of the straight lines in Fig. 7 determine the frequency factors and activation energies, respectively. Table III lists these kinetic parameters under mixed rate-controlling condition for oxidations with H_2O(g), CO–CO_2 gas mixtures and pure CO. It is noted from these results that, under the mixed rate-controlling regime, the activation energy for Si_3N_4-bonded SiC oxidation in CO or CO–CO_2 gas mixtures is larger than that in H_2O(g). However, the activation energy for all the oxidants is less than that in air (155.99 kJ mol^{-1}) [3]. The possible reason for this is that flowing oxidants were employed in this work, improving the kinetic conditions (diffusion through the product layer) for Si_3N_4-bonded SiC oxidation whereas, with air oxidation, a still-air configuration was used.

Fig. 9 shows a plot of the Thiele modulus, φ^2, as a function of temperature. It is seen that, as the temperature increases, the Thiele modulus decreases for all oxidants, which means that the increase in reaction rate is slower than the decrease in diffusion resistance with increasing temperature. This is attributed to the crystallization of SiO_2 at higher temperatures which slows down the intrinsic reaction. Fig. 10 gives the influence of CO volume composition on the Thiele modulus. It shows that the CO concentration has a significant effect on φ^2 within a concentration range of less that 20 wt%. When CO reaches the concentration typically prevailing in the blast furnace environment, φ^2 approximately approaches a constant

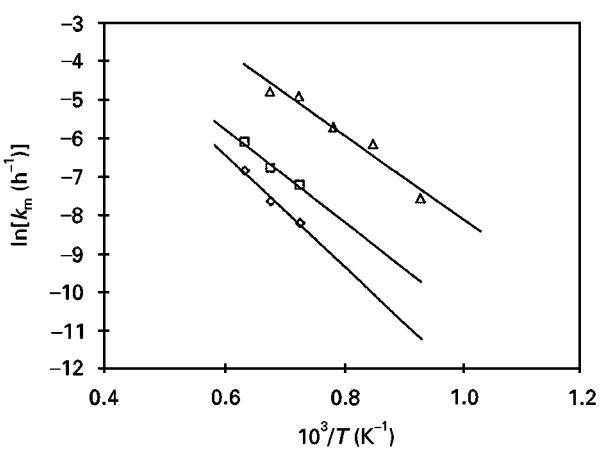

Figure 8 Arrenhius plots for various oxidants. (◇), CO; (□), CO–CO_2(CO-to-CO_2 ratio, 3 to 1); (△), H_2O(g).

TABLE III Kinetic parameters under the mixed rate-controlling condition

Oxidant	Temperature (K)	Activation energy, E (kJ mol^{-1})	Frequency factor, A_0 (h^{-1})	Regression coefficient
H_2O(g)	1073–1573	90.99	17.992	0.953
CO–CO_2 (CO-to-CO_2 ratio, 3 to 1)	1373–1573	100.15	4.529	0.973
Pure CO	1373–1573	121.21	10.716	0.982

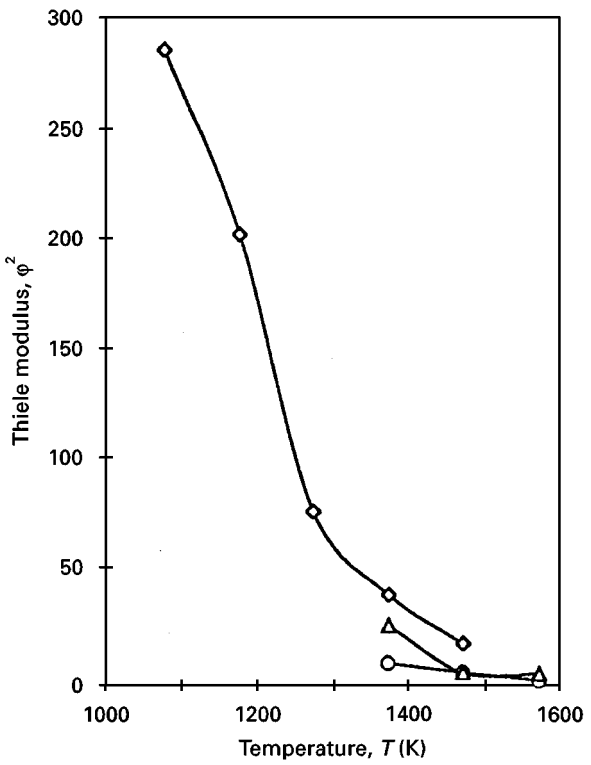

Figure 9 Thiele modulus as a function of temperature for various oxidants. (◇), H_2O(g); (○), CO; (△), CO–CO_2 (CO-to-CO_2 ratio, 3 to 1).

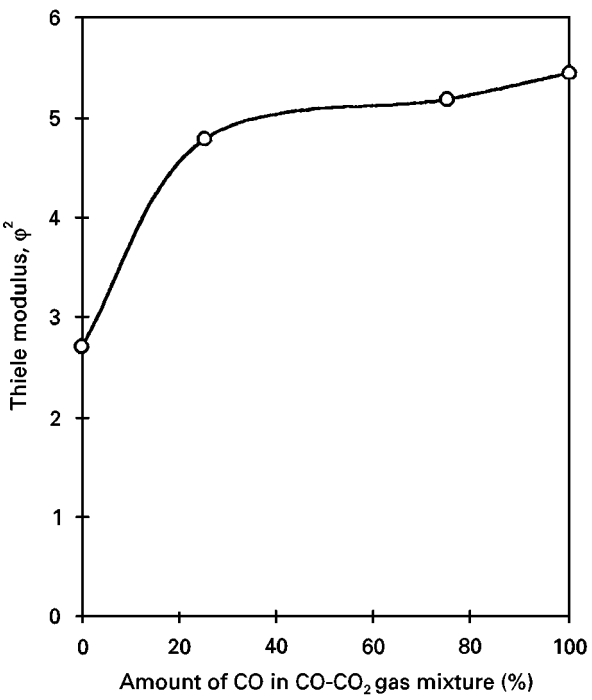

Figure 10 Effect of CO concentration on the Thiele modulus at 1473 K.

($\varphi^2 \approx 5$). This indicates that the oxidation of Si_3N_4-bonded SiC bricks under blast furnace conditions is in the mixed rate-controlling regime but is dominated by chemical reaction.

5. Conclusion

In this paper, a thermodynamic analysis is presented on the oxidation mechanisms (active and passive oxidation) of Si_3N_4-bonded SiC bricks, with respect to blast furnace conditions. The transition from passive to active oxidation was also investigated through thermodynamic simulations. It was found that, under the blast furnace atmosphere, Si, SiC and Si_3N_4 were simultaneously oxidized passively to SiO_2 by CO, CO_2 and water vapour. This further confirms that Si_3N_4-bonded SiC bricks can be used safely in blast furnaces with SiO_2 as a protection layer against further oxidation.

Three kinetic rate-controlling expressions are used to fit the experimental data of the weight gain versus time. It was found that the mixed rate-controlling mechanism of both reaction and diffusion best describe the oxidation kinetics of this ceramics in pure CO, CO–CO_2 gas mixtures and H_2O(g). The activation energy for Si_3N_4-bonded SiC oxidation in CO or CO–CO_2 gas mixtures is larger than that in H_2O(g), but the activation energies for all these oxidants are less than that for oxidation in air.

References

1. A. FICHEL and J. RRAMSS, *Interceram* **2** (1983) 38.
2. C. L. KERAN and R. W. BROWN, *Iron and Steel Eng.* **12** (1987) 35.
3. B. PEI, G. Q. (MAX) LU and G. X. WANG, *Ceram. Trans.* **44** (1994) 253.
4. J. W. KAUFMAN, D. CAMPOS-LORIZ, K. R. SELKREGG and T. R. HOLMES, *Interceram* **4** (1983) 8.
5. M. CHASE, C. DAVIES, J. DOWNEY, D. FRURIP, R. MCDONALD and A. SYVERUD, "JANAF thermodynamic tables" (American Chemical Society, American Institute of Physics, New York, 3rd Edn, 1986).
6. E. A. GULBRANSEN and S. A. JANSSON, *Oxid. Metals* **4** (1972) 181.
7. A. H. HEUER and V. L. K. LOU, *J. Amer. Ceram. Soc.* **73** (1990) 2785.
8. G. ERIKSSON, *Chem. Scripta* **8** (1975) 100.
9. C. WAGNER, *J. Appl. Phys.* 29 (1958) 1295.
10. R. B. BIRD, W. E. STEWART and E. N. LIGHTFOOD, "Transport phenomena" (Wiley, New York, 1960) pp. 508–513.

11. M. BALET, G. FLAMANT, G. MALE and G. PICHELIN, *J. Mater. Sci.* **27** (1992) 697.
12. J. SZEKELY, J. W. EVANS and H. Y. SOHN, "Gas–solid reactions" (Academic Press, New York, 1976) p. 76.
13. D. Y. PENG, J. H. LI, S. Z. LIU, Y. YU, Y. L. WANG and Z. T. WANG, in "Properties and application of Si_3N_4-bonded SiC bricks for blast furnaces", United International Technical Conference on Refractories 1–4 November 1989, Anaheim, UNITECR'89 Proceedings, Vol. 1, edited by L. J. Trostel (American Ceramic Society, Columbus, OH, 1989) pp. 101–108.
14. J. A. COSTELLO and E. TRESSLER, *J. Amer. Ceram. Soc.* **64** (1981) 327.
15. D. J. CHOI, D. B. FISCHBACK and W. D. SCOTT, *ibid.* **72** (1989) 1118.
16. K. L. LUTHRA, *ibid.* **74** (1991) 1095.

Received 11 November 1996
and accepted 14 October 1997